Inorganica Chimica Acta, *84* (1984) 95–100

μ_3-S Bonding Mode in $H_2M_3(CO)_9S$ Clusters of Ru and Os. An UV–PES and Theoretical Study

GAETANO GRANOZZI*, RENZO BENONI, MARIO ACAMPORA

Istituto di Chimica Generale ed Inorganica, Università di Padova, Via Loredan 4, 35100 Padua, Italy

SILVIO AIME and DOMENICO OSELLA

Istituto di Chimica Generale ed Inorganica, Università di Torino, Corso M. D'Azeglio 48, Turin, Italy

Received July 14, 1983

The electronic structure of $H_2M_3(CO)_9S$ clusters (M = Ru, Os) is discussed on the basis of their He I and He II excited gas-phase photoelectron spectra and on the basis of CNDO quantum mechanical calculations. The PE data clearly demonstrate the cleavage of two direct M–M interactions by operation of the bridging hydrides, giving rise to three-center two-electron M–H–M levels. The μ_3-S bonding mode has been described in detail and compared with previous results on related μ_3-CY cluster derivatives. The CNDO results on $Ru_3(CO)_9S^{=}$, $HRu_3(CO)_9S^-$ and $H_2Ru_3(CO)_9S$ indicate that the μ_3-S–cluster interaction is mostly independent of the presence of the bridging hydrides.

Introduction

Sulfur-bridged derivatives of transition metal carbonyl clusters have been characterized long ago, and today a variety of structural arrangements are known [1] in which the sulfur atoms can act as a $2e^-$, $3e^-$ or $4e^-$ donor, namely

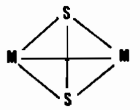

A

(2e⁻ donor)

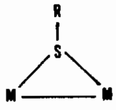

B

(3e⁻ donor)

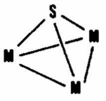

C

(4e⁻ donor)

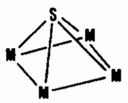

D

(4e⁻ donor)

Recently, S bridged species have been used as intermediates for the synthesis of high-nuclearity carbonyl clusters, and the sulfur atoms, by virtue of adaptable coordination numbers, have been recognized to assist in the growth of large clusters through aggregation of metallic fragments [2]. Furthermore, sulfur is a severe poison for several catalysts [3] and it has been suggested that atomic sulfur is chemisorbed on the Ni(111) crystal face as a μ_3-bridging species [4]. A better knowledge of the bonding mode of sulfur with several metallic centers will then provide information of some chemical relevance.

The electronic structure and the gas-phase UV photoelectron (PE) spectra of derivatives of type A and B have been already reported [5–7]. In particular, the $Fe_2(CO)_6S_2$ molecule has been the object of several theoretical [5, 8] and PE studies [5, 6]; Van Dam *et al.* [5], on the basis of *ab initio* calculations, proposed that the bonding of the briding S_2 ligand occurs mainly through the donation of electrons from the $Fe_2(CO)_6$ moiety to empty orbitals of the bridging ligand. We recently examined PE spectra of $H(SR)Os_3(CO)_{10}$ derivatives [7] where the B type coordination mode is present.

We report here the He I and He II excited PE spectra of $H_2M_3(CO)_9S$ (M = Ru, Os), as being representative of the μ_3-S coordination mode C.

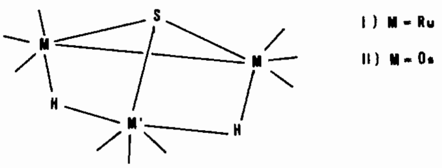

CNDO type calculations have been also used as a theoretical aid to discuss the PE data in order to gain more insights into the bonding scheme; more

---

*Author to whom correspondence should be addressed.

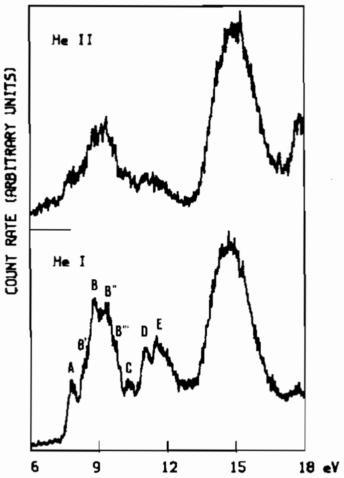

Fig. 1. He I and He II PE spectra of $H_2Ru_3(CO)_9S$.

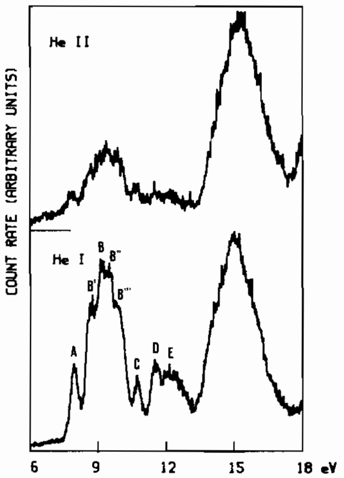

Fig. 2. He I and He II PE spectra of $H_2Os_3(CO)_9S$.

accurate quantum chemical methods are precluded by their molecular complexity.

The aim of this work was oriented to assess the following points:

(i) The bonding scheme relative to the μ_3-S coordination mode in comparison with that previously reported for μ_3-CY [9, 10];

(ii) The role of H bridges with regard to the metal–metal and cluster–sulfur interactions;

(iii) The charge density distribution within the whole cluster framework.

Experimental

Preparation

Both complexes $H_2Ru_3(CO)_9S$ (I) and $H_2Os_3(CO)_9S$ (II) have been synthesized by direct reaction of $Ru_3(CO)_{12}$ and $Os_3(CO)_{12}$ respectively with H_2S, according to the literature methods [11, 12]. Their purity was checked by IR and MS spectroscopy.

PE Spectroscopy

He I (21.217) and He II (40.814) excited PE spectra were run on a Perkin-Elmer PS-18 spectrometer using a heated inlet probe system. They were recorded in the 70–100 °C temperature range and no decomposition evidence has been observed. The spectrometer was connected on-line with a Minc-23 computer (Digital Eq.). Data acquisition was carried out by 5–6 sweeps over 500 distinct channels, each sweep amounting to *ca.* 5 minutes. The ionization energy (IE) scale was calibrated by reference to peaks due to mixed inert gases (Xe, Ar) and to $1S^{-1}$ He ionization. The IEs reported in Table I are the mean values over several distinct runs.

Calculations

Quantum mechanical calculations were performed by a version of the CNDO method [13] suitable for transition metal complexes. Ru semi-empirical parameters were obtained [13] from atomic spectroscopical data, whereas the C, O, H and S parameters are Pople's standards [14]. The geometrical data used in the calculation refer to the X-ray structural determination of I [11]. The molecule contains a mirror plane and the MOs are labelled according to the C_s point group. The computed eigenvalues were related to the measured IEs assuming the validity of the Koopmans' theorem [15]. Gross atomic charges and overlap populations were obtained by Mulliken's population analysis [16] of the de-orthogonalized [17] eigenvectors.

Results and Discussion

PE Data

The He I and He II excited gas-phase PE spectra of I and II are shown in Figs. 1 and 2 respectively and the pertinent IEs are reported in Table I.

In the lowest IE region (up to 13.5 eV of the He I spectra) both I and II present four well-resolved bands labelled as A, C, D and E in the Figs. and a broad band B with several components (shown as B′, B″, B‴). Minor differences between I and II, however, are evident as far as the relative intensity of bands A, B and C with respect to the higher IE bands. In particular, the increased intensities in II is certain to be related to the larger He I photoionization cross-section of 5d orbitals with respect to 4d ones ('heavy metal effect') [18], and this experimental evidence furnishes information in order to recognize the bands related to ionizations from MOs mainly

TABLE I. Experimental Ionization Energies (eV) of the Studied Clusters.

Band	$H_2Ru_3(CO)_9S$	$H_2Os_3(CO)_9S$
A	7.80	8.09
B'	8.38	8.88
B	8.81	9.31
B''	9.31	9.62
B'''	9.77	9.96
C	10.28	10.78
D	11.08	11.55
E	11.54	12.18

localized on the metallic framework. Further information is obtained by the analysis of the He I/He II intensity changes (Figs. 1 and 2): the marked decrease of bands D and E is to be related to high contributions from hydrogen 1s and/or sulfur 3p AOs to the corresponding MOs, due to their very low photoionization cross-section at the He II wavelength [19].

The spectral region beyond 13.5 eV consists of a very broad and unresolved envelope, mostly due to ionizations from levels localized on the carbonyl framework (5σ, 1π and 4σ MOs of free carbon monoxide). This broad band prevents the detection in this region of resolved bands pertaining to MOs not localized on the carbonyl groups. Further analysis of this region is not productive and we shall confine ourselves to the discussion of the lower IE region.

In this section we will discuss qualitatively the PE data on the basis of experimental criteria and comparison arguments with previously reported related molecules. In particular, the recent PE data on several trimetallic clusters of Ru and Os [7, 20–22] have shown that the lower IE region (up to 13.5 eV) can be divided into three parts, which correspond to ionizations with a peculiar predominant character, *i.e.* metal–metal bonding, metallic 'nd' non-bonding, and cluster–substrate bonding.

Band A in both I and II is assigned to ionization from a metal–metal bonding level: their IEs are very similar to those found in triangular clusters containing three or two direct metal–metal interactions [7, 20–22]. It is interesting to note, however, that in the present case one well-resolved and sharp band has to be attributed to just one direct metal–metal bonding level. Band B (with its shoulders) and band C are related to ionizations from MOs largely localized on the metal atoms with predominant non-bonding 'nd' character (referenced as 't_{2g}-like' because of their parentage with pseudo-t_{2g} orbitals of a $M(CO)_4$ fragment [23]). As previously shown [7, 24] the ionizations within the 't_{2g}-like' set can be split into several components according to the geometrical arrangement of the metallic framework and the nature of the bridging ligands. Actually, the band labelled as C in Figs. 1 and 2 is always present at the same IE in the spectra of all the trinuclear clusters

TABLE II. CNDO Results for $H_2Ru_3(CO)_9S$.

MO	ε (eV)	pop., %					dominant character
		Ru		S	2H	9CO	
		Ru3	Ru1,2				
28a'' (LUMO)	+2.09	19	68	2	0	11	Ru1–Ru2 antibonding
34a' (HOMO)	−6.07	1	87	2	0	10	Ru1–Ru2 bonding
33a'	−7.53	24	48	16	4	8	't_{2g}-like' non-bonding metallic levels with some mixture of sulfur and π* CO orbitals
27a''	−7.78	18	59	12	7	4	
32a'	−7.91	18	59	14	0	9	
26a''	−8.03	4	86	1	0	9	
25a''	−8.37	15	76	0	0	9	
24a''	−8.41	23	59	7	1	10	
31a'	−8.46	32	57	0	1	10	
30a'	−8.76	51	38	2	0	9	
29a'	−9.17	54	36	1	2	7	
23a''	−9.25	48	25	2	15	10	Ru3 $\overset{\text{H}}{\wedge}$ Ru1,2 bonding
28a'	−9.41	41	30	2	12	15	
27a'	−10.58	12	31	46	1	10	'e-like' S-cluster bonding
22a''	−10.98	24	20	40	6	10	
26a'	−13.04	13	20	54	6	7	'a_1-like' S-cluster bonding

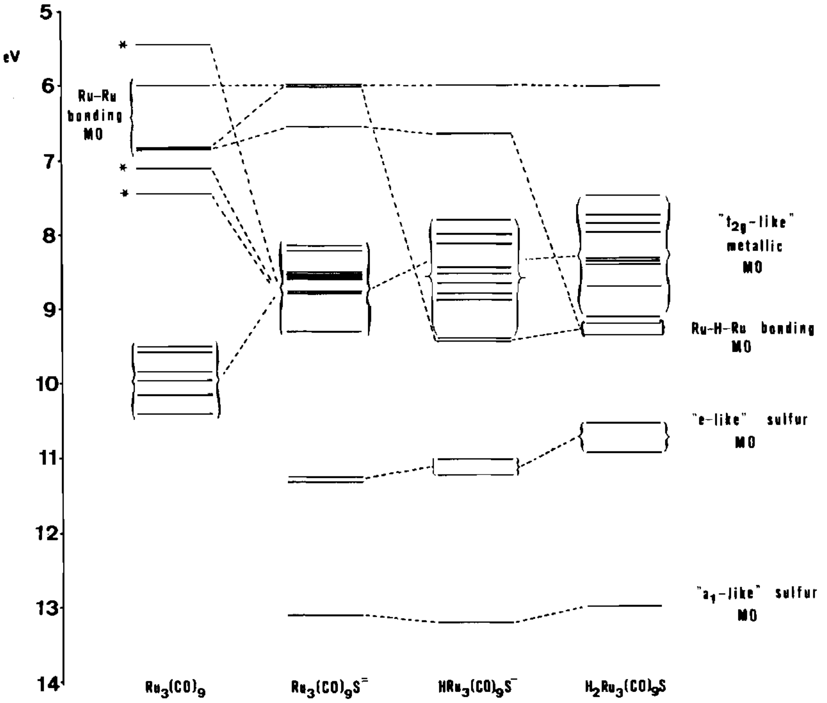

Fig. 3. CNDO correlation diagram between $Ru_3(CO)_9$, $Ru_3(CO)_9S^{=}$, $HRu_3(CO)_9S^-$ and $H_2Ru_3(CO)_9S$.

containing a $M_3(CO)_9$ subunit [21, 22]. In our opinion this feature is evidence to assign band C to a 't_{2g}-like' level representing a stabilized in-phase combination of metallic 'nd' orbitals.

Bands D and E are to be related to M–H–M and M_3–S bonding levels. However, experimental criteria are not sufficient to assign the two bands with enough confidence. The theoretical results reported in the next section will allow us to discuss the bonding scheme and the assignment in more detail.

Theoretical Results

On the basis of the empirical EAN rule, the title compounds can be qualitatively described as 48-electron saturated clusters when the sulfur atom is considered as a four electron donor. This qualitative method, however, cannot give information about the actual electronic distribution. Qualitative analyses of the μ_3-S bonding scheme have been already reported for the related paramagnetic $Co_3(CO)_9S$ molecule [25, 26]; however, in this case, the emphasis was on the localization of the unpaired electron and the discussion of the bonding of the whole cluster has been limited to symmetry considerations.

CNDO computed eigenvalues and eigenvectors of the 15 outermost occupied MOs and of the LUMO of $H_2Ru_3(CO)_9S$ are reported in Table II. As already noted in previous studies [20, 21], the CNDO method reproduces the major PE spectral features (within the Koopmans' theorem [15]). In fact, the assignment of the PE spectra discussed in the previous section on the basis of purely comparative experimental arguments are fully confirmed by the results of Table II, where the predominant character of each MO is also shown. In particular the HOMO 34a′, well distinct in energy from the subsequent MOs, relates to the non-bridged Ru1–Ru2 bond and is assigned to the band A of Figs. 1 and 2. The subsequent nine MOs, largely localized on the metal centers, are associated to the 't_{2g}-like' bands B and C whereas the 23a″, 28a′, 27a′, 22a″ MOs, with high contributions from S and H atoms, are related to bands D and E. The only discrepancy between the computed and experimental IEs consists in the energy spacing between the Ru–H–Ru and Ru_3–S bonding MOs. According to the theoretical results, the ionization associated to the inner 26a′ Ru_3–S bonding orbital should be expected under the broad band due to the carbonyl ionizations at higher IE.

It is worth noting that the CNDO computed LUMO 28a″ (Table II) has a metal–metal antibonding character, in agreement with the results obtained for the localization of the further unpaired electron in the related $Co_3(CO)_9S$ molecule [25, 26].

A more detailed picture of the bonding scheme is obtained by reference to Fig. 3 where a correlation diagram between the outmost MOs of the $Ru_3(CO)_9$, $Ru_3(CO)_9S^{=}$, $HRu_3(CO)_9S^-$ and $H_2Ru_3(CO)_9S$ sys-

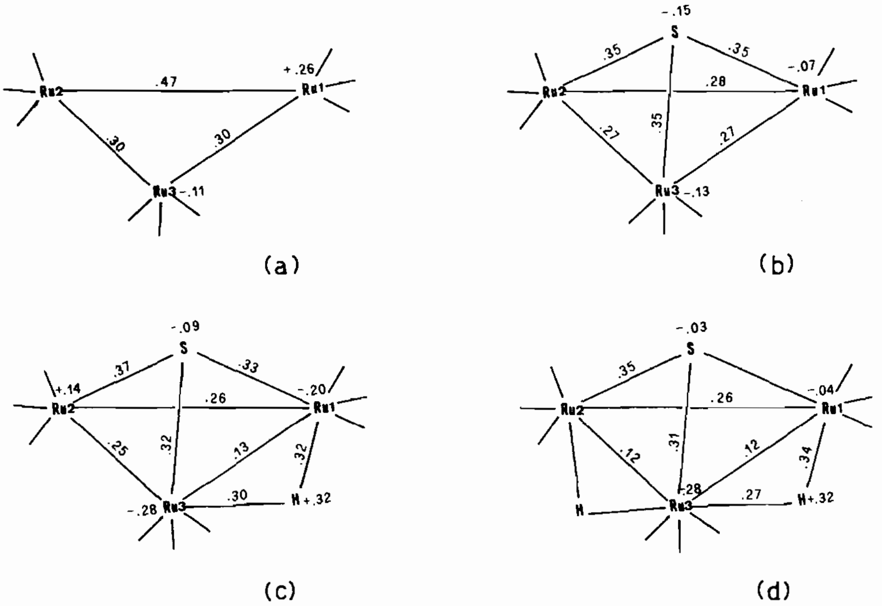

Fig. 4. CNDO gross atomic charges and overlap populations for $Ru_3(CO)_9$ (a), $Ru_3(CO)_9S^=$ (b), $HRu_3(CO)_9S^-$ (c) and $H_2Ru_3(CO)_9S$ (d).

tems is reported. The geometry of the fragments has been kept frozen as in the dihydride cluster* and the energy levels have been shifted in order to match the energy of the outmost Ru–Ru bonding MO in the fragments.

The $Ru_3(CO)_9$ fragment shows three high-lying 't_{2g}-like' levels (in the same region of the three Ru–Ru metal bonds and labelled with an asterisk in Fig. 3) which are suitable to donate charge to the μ_3-S atom**. A clear description of the interaction involving the sulfur atom is obtained by the comparison with the levels of $Ru_3(CO)_9S^=$. The 't_{2g}-like' levels now span over a small energy range because of stabilization of the high-lying levels and destabilization of the inner ones. This reflects respectively a charge donation from $Ru_3(CO)_9$ to virtual AOs of the sulfur atom and a mixing of the filled inner sulfur orbitals with 't_{2g}-like' cluster levels which are close in energy.

The former mechanism explains the high sulfur contribution to the 33a′, 27a″ and 32a′ MOs shown in Table II. The inner sulfur based MOs are grouped in two sets which relate to 'e-like' and 'a_1-like' in an ideal C_{3v} symmetry; the bonding scheme is very similar to that previously proposed for the CY fragment over a metallic triangle [9, 10]. A remarkable difference, however, is found for the energy of this 'e-like' bonding level: in $H_3Ru_3(CO)_9CY$ [10] this 'e-like' level lies at higher energy with respect to the 't_{2g}-like' metallic levels, whereas in the present case and in $Co_3(CO)_9CY$ [9] this 'e-like' orbital lies at lower energy.

The major effect (Fig. 3) of interaction with one ($HRu_3(CO)_9S^-$) or two hydrogen atoms ($H_2Ru_3(CO)_9S$) is the cleavage of one or two Ru–Ru bonds giving rise to lower-lying Ru–H–Ru bonding MOs. The perturbation of H-bridges on the Ru_3–S bonding system can be considered negligible.

The atomic gross charges and overlap populations (Fig. 4) obtained by Mulliken's population analysis of the CNDO eigenvectors provide further insight into the electronic charge distributions. This analysis is of particular significance when carried out in a comparative way, such as that employed in Fig. 4 where the data for the various fragments are compared. Let us follow the building up of the cluster from the fragments (Fig. 4): in the frozen $Ru_3(CO)_9$ unit (Fig. 4a) there is a large charge unbalance between the metal centers because of the non-equivalent Ru–Ru distances (see the corresponding overlap populations). The presence of the sulfur atom (Fig. 4b) balances the metallic atomic charges by means of selective interactions: the Ru1 and Ru2 atoms gain charge by a strong charge donation from sulfur into a Ru1–Ru2 antibonding level (see the

---

*In our opinion this procedure eliminates arbitrariness in the choice of the geometry of the fragments and furnishes a better description of the interaction pattern.

**These pending MOs arise from the peculiar geometrical arrangement of the fragment. When the ideal C_{3v} geometry is assumed, results very similar to those obtained by Schilling *et al.* [27] and Sherwood *et al.* [24] are reproduced.

reduction of the Ru1–Ru2 overlap population*). However, the observation that the three Ru–S and Ru–Ru overlap populations are eventually equivalent (Fig. 4b) shows that the sulfur–cluster interaction is not far from a C_{3v} symmetric description. The introduction of the hydrogen atom (Fig. 4c and 4d) draws charge at the bridged metallic edges and markedly reduces the corresponding Ru–Ru overlap populations. Both these facts are the consequence of the mentioned conversion of Ru–Ru bonding MOs into three-center two-electron Ru–H–Ru orbitals. As a consequence, the sulfur atomic charge reduces progressively whereas no significant variation in the Ru–S overlap populations is found.

These findings are supported by the diffraction studies of the related clusters $HOs_3(CO)_9S^-$ (X-ray) [28] and $H_2Os_3(CO)_9S$ (II) (X-ray and neutron) [29]. In the anion there are two short and one long (probably hydride-bridged) Os–Os distances; in the parent cluster there are one short and two long (hydride-bridged) Os–Os bonds; however the mean Os–S distances in the two molecules are almost identical.

Acknowledgements

Thanks are due to the Ministero della Pubblica Istruzione (Grant M.P.I. 12/2/15) for support of this work and to Prof. E. Tondello for helpful suggestions.

References

1 H. Vahrenkamp, *Angew. Chem. Internat. Edit.*, *14*, 322 (1975).
2 R. D. Adams, I. T. Horwarth and L. W. Yang, *J. Am. Chem. Soc.*, *105*, 1533 (1983).
3 L. Marko, *Gazz. Chim. Ital.*, *109*, 247 (1979).
4 J. E. Demuth, D. W. Japson and P. M. Marcus, *Phys. Rev. Lett.*, *32*, 1182 (1974).
5 H. Van Dam, J. N. Louwen, A. Oskam, M. Doran and I. H. Hillier, *J. Electron Spectrosc. Relat. Phenom.*, *21*, 57 (1980).
6 E. L. Anderson, T. P. Fehlner, A. E. Foti and D. R. Salahub, *J. Am. Chem. Soc.*, *102*, 7422 (1980).
7 G. Granozzi, R. Benoni, E. Tondello, M. Casarin, S. Aime and D. Osella, *Inorg. Chem.*, 22, (1983).
8 B. K. Teo, M. B. Hall, R. F. Fenske and L. F. Dahl, *Inorg. Chem.*, *14*, 3103 (1975).
9 G. Granozzi, E. Tondello, D. Ajò, M. Casarin, S. Aime and D. Osella, *Inorg. Chem.*, *21*, 1081 (1982).
10 D. E. Sherwood Jr. and M. B. Hall, *Organometallics*, *1*, 1519 (1982).
11 R. D. Adams and D. A. Katahira, *Organometallics*, *1*, 53 (1982).
12 A. J. Deeming and M. Underhill, *J. Organomet. Chem.*, *42*, 660 (1972).
13 E. Tondello, *Inorg. Chim. Acta*, *11*, L5 (1974).
14 J. A. Pople and G. A. Segal, *J. Chem. Phys.*, *44*, 3289 (1966).
15 T. C. Koopmans, *Physica*, *1*, 104 (1934).
16 R. S. Mulliken, *J. Chem. Phys.*, *23*, 1833 (1955).
17 P. O. Löwdin, *J. Chem. Phys.*, *18*, 365 (1950).
18 B. R. Higginson, D. R. Lloyd, P. Borroughs, D. M. Gibson and A. F. Orchard, *J. Chem. Soc. Faraday II*, *69*, 1659 (1973).
19 J. W. Rabalais, 'Principles of UV Photoelectron Spectroscopy', Wiley Interscience, (1977).
20 D. Ajò, G. Granozzi, E. Tondello and I. Fragalà, *Inorg. Chim. Acta*, *37*, 191 (1979).
21 G. Granozzi, E. Tondello, R. Bertoncello, S. Aime and D. Osella, *Inorg. Chem.*, *22*, 744 (1983).
22 G. Granozzi, R. Bertoncello, S. Aime and D. Osella, *J. Organomet. Chem.*, *229*, C27 (1982).
23 M. Elian and R. Hoffmann, *Inorg. Chem.*, *14*, 1058 (1975).
24 D. E. Sherwood, Jr., and M. B. Hall, *Inorg. Chem.*, *21*, 3458 (1982).
25 C. E. Strouse and L. F. Dahl, *J. Am. Chem. Soc.*, *93*, 6032 (1971).
26 M. H. Chisholm and I. P. Rothwell, *Progr. Inorg. Chem.*, *29*, 1 (1982).
27 B. E. R. Schilling and R. Hoffmann, *J. Am. Chem. Soc.*, *101*, 3456 (1979).
28 B. F. G. Johnson, J. Lewis, D. Pippard and P. Raithby, *Acta Cryst.*, *B24*, 3767 (1978).
29 B. F. G. Johnson, J. Lewis, D. Pippard, P. Raithby, G. M. Sheldrick and K. D. Rouse, *J. Chem. Soc. Dalton*, *616* (1979).

---

*Actually the 26a" LUMO of $Ru(CO)_9$ is almost uniquely localized on Ru1 and Ru2 (*ca.* 80%).